4-17-2019

Adsorption of Organic Micropollutants to Biosolids-Derived Biochar: Estimation of Thermodynamic Parameters

Yiran Tong
Marquette University

Brooke K. Mayer
Marquette University, Brooke.Mayer@marquette.edu

Patrick J. McNamara
Marquette University, patrick.mcnamara@marquette.edu

Adsorption of Organic Micropollutants to Biosolids-Derived Biochar: Estimation of Thermodynamic Parameters

Yiran Tong
Department of Civil, Construction and Environmental Engineering, Marquette University, Milwaukee, WI
Brooke K. Mayer
Department of Civil, Construction and Environmental Engineering, Marquette University, Milwaukee, WI
Patrick J. McNamara[*]
Department of Civil, Construction and Environmental Engineering, Marquette University, Milwaukee, WI

*Corresponding author
Email:Patrick.McNamara@marquette.edu
Phone: 414-288-2188

Keywords

Adsorption enthalpy; Adsorption free energy; Pyrolysis; Mechanisms; Wastewater; Reuse

Abstract

This research quantified thermodynamic parameters to better understand the use of wastewater biosolids-derived biochar as an adsorbent to remove micropollutants. The objective of this research was to quantify adsorption capacity; isosteric heat; and change of enthalpy, entropy, and free energy characterizing adsorption reactions between biochar and micropollutants. Adsorption isotherms were developed using a range of temperatures for the micropollutants benzyldimethyldecylammonium chloride (BAC-C10) Carbamazepine (CBZ), 17β-estradiol (E2), 17α-ethynylestradiol (EE2), and triclosan (TCS). The thermodynamic parameters derived from the isotherm data were used to assist in characterizing binding affinity, spontaneity, and mechanisms of adsorption. More polar compounds such as BAC-C10 and CBZ exhibited linear adsorption, indicating weak interactions with more polar amorphous moieties on the biochar surface. For the micropollutants that were present predominantly in the neutral form at pH 7 (CBZ, E2, EE2, and TCS), increasing hydrophobicity increased the extent of adsorption. The enthalpy change of adsorption and the positive correlation between hydrophobicity and change of entropy ($R^2 = 0.8$) both suggest that hydrophobic interaction was the dominant adsorption mechanism for neutral compounds. Increases in adsorption with increasing temperature, together with the estimated thermodynamic parameters, indicated that the reactions were endothermic, meaning that higher temperatures should offer improved removal via adsorption. The negative free energy changes observed suggested that adsorption was spontaneous and that adsorption rates outcompete desorption rates. Under multi-solute conditions, the adsorption capacities for all compounds were suppressed to varying extents; however, the magnitude of changes in enthalpy and entropy were not affected by competitive multi-solute adsorption.

1. Introduction

An emerging issue facing Water Resource Recovery Facilities (WRRFs) is the increasing presence of organic micropollutants derived from anthropogenic activities, such as pharmaceuticals, hormones, and antimicrobials [1,2]. Conventional WRRFs are a major source of organic micropollutants entering the environment because conventional treatment processes were not designed to remove these compounds [3,4]. Although WRRFs discharge micropollutants at low concentrations (ng/L to µg/L), complex mixtures of multiple micropollutants can have synergistic impacts on biological systems [5]. Fish feminization stemming from chronic exposure to estrogenic compounds has been well-documented [6,7]. Biologically active micropollutants, including antibiotics and antimicrobials, can also select for antibiotic resistance in natural and engineered environments [8–13]. More efficient micropollutant removal beyond that provided by conventional treatment processes is needed.

Reverse osmosis and advanced oxidation processes (AOPs), including UV treatment with hydrogen peroxide or ozone, provide high micropollutant removal efficiencies, but these processes require high energy inputs [14–16]. In the Nutrient-Energy-Water (NEW) paradigm used to guide sustainable WRRF planning, resource recovery and production of value-added products are paramount. High-energy processes such as AOPs can make it difficult for WRRFs to achieve energy neutrality, whereas micropollutant adsorption may offer a potentially low-cost, viable alternative. Activated carbon has been shown to effectively remove micropollutants such as benzotriazole, carbamazepine, and sulfamethoxazole [17,18].

Biochar is another type of adsorbent material that could be used to remove micropollutants. Pyrolysis of wastewater biosolids can produce biochar on site for subsequent use as a micropollutant adsorbent as part of an internal WRRF recycle loop [19–25]. After micropollutant adsorption, biosolids-derived biochar could be recycled back into the pyrolysis process [26,27] since pyrolysis removes micropollutants, including antimicrobials, antibiotics, estrogenic hormones, and antibiotic resistance genes [28–30]. Additionally, excess biochar can be used as an effective soil amendment [23,31,32]. Beyond biochar, pyrolysis offers potential to recover energy from biosolids in the form of pyrolysis gas, which can be co-combusted with anaerobic digester bio-gas [33,34]. Therefore, depending on the water content of the biosolids, pyrolysis can be energy positive [21]. Accordingly, pyrolysis of wastewater

biosolids could offer a self-sustaining means of recovering energy from biosolids while facilitating the removal of micropollutants from wastewater via adsorption.

Previous studies have demonstrated that biochar can adsorb some micropollutants [22,24–26], but fundamental investigation of the thermodynamic profiles characterizing interactions between biosolids-derived biochar and neutral/ionic micropollutants has not been reported. Thermodynamic profiles, including isosteric heat (ΔH_{st}) and changes of standard enthalpy (ΔH^0), entropy (ΔS^0), and free energy (ΔG^0) can be used to better understand the effectiveness of organic micropollutant adsorption using biosolids-derived biochar. Specifically, thermodynamic profiles are needed to elucidate binding mechanisms [17,22,35,36], which can inform subsequent process optimization.

Several studies have estimated thermodynamic parameters for adsorption of micropollutants using plant-derived biochars [37–40]. For example, Vithanage et al. (2016) reported a negative ΔG^0 for adsorption of carbofuran on tea waste-biochar, reflecting that adsorption did not require an external energy input. The ΔH^0 was -46 kJ/mol, indicating the exothermic nature of the adsorption and weak physical interaction [39]. Adsorption of other organic pollutants from aqueous phase onto biochar is characterized as endothermic by positive ΔH^0 values.. For example, Chen et al.[40] estimated the change of enthalpy for 1,3-dinitrobenzene and naphthalene adsorption on pine needle-derived biochar as 14 kJ mol^{-1} and 16 kJ mol^{-1}, respectively. However, little is known about the thermodynamic profiles for micropollutant adsorption to biosolids-derived biochar. Knowledge of the thermodynamic parameters characterizing adsorption can provide insight into the spontaneity of adsorption, adsorption mechanisms, and the adsorbent surface properties.

The objective of this research was to generate thermodynamic profiles for adsorption of a suite of micropollutants onto biosolids-derived biochar. The micropollutants selected for this study were carbamaze[ome (CBZ), 17β-estradiol (E2), 17α-ethinylestradiol (EE2), triclosan (TCS), and benzyldimethylammonium chloride (BAC-C10). These micropollutants were selected as study targets because they are frequently detected in treated wastewater effluents [41,42] and encompass a wide variety of chemical properties (Table 1). In circumneutral pH wastewater, CBZ (pK_a=13.9, $logK_{ow}$=2.45), E2 (pK_a=10.7, $log K_{ow}$=3.94), and EE2 (pK_a=10.3, $logK_{ow}$=3.67) are hydrophobic, neutral molecules. In this same pH range, TCS can be present as either an anion or neutral molecule (pK_a =7.9, $logK_{ow}$=4.76), while BAC dissociates as a permanent cation in water. Anionic compounds were not included in this study as they reportedly do not adsorb well to the biosolids-derived biochar used here [27]. Thermodynamic analysis of batch adsorption data was conducted using a range of experimental temperatures to 1) establish the impact of temperature on adsorption capacities, and 2) derive and compare binding energies among representative micropollutants. Potential binding mechanisms were elucidated from the thermodynamic profiles.

2. Experimental Approach

2.1 Biosolids-derived biochar production and pre-conditioning

Bench-scale batch experiments were conducted to determine the adsorption capacities for micropollutants on biosolids-derived biochar by developing isotherms at a range of reaction temperatures. Thermodynamic profiles of biochar adsorption were then derived from the isotherms for the suite of micropollutants. Finally, the impacts of competition from other micropollutants were evaluated.
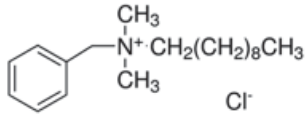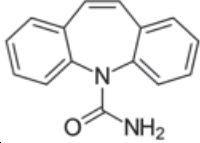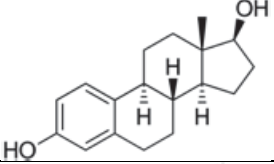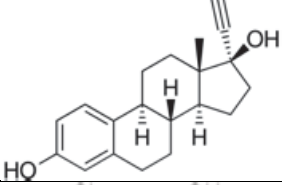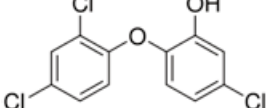
A heat-dried blend of anaerobically digested primary solids and waste activated sludge produced by the Milwaukee Metropolitan Sewage District (MMSD) in Milwaukee, WI, was used as pyrolysis feedstock. The feedstock was pyrolyzed to produce biochar in accordance with the method described by Tong et al. [22]. Briefly, biosolids were purged with argon gas in a flask for 15 min, and then pyrolyzed at 600°C for 1 hour. The resulting biochar was treated with 1 M HCl to reduce ash content and increase surface area [22]. The dried treated biochar

particles were sieved to approximately 1.4 mm in diameter (sieve mesh No. 14) for use in subsequent adsorption experiments. In previously published work, surface characterization of biochar derived from the same source was presented [22,43].

2.3 Adsorption batch experiments

BAC-C10 (97%, Sigma Aldrich, St. Louis, MO), CBZ (97%, Sigma Aldrich, St. Louis, MO), E2 (97%, Sigma Aldrich, St. Louis, MO), EE2 (97%, Sigma Aldrich, St. Louis, MO), and TCS (97%, Sigma Aldrich, St. Louis, MO) were pre-dissolved in HPLC-grade methanol for use as feedstock solutions. The physical and chemical properties of the compounds are listed in Table 1. Reaction solutions were prepared by adding each micropollutant individually (or as a mixture of all micropollutants for multi-solute experiments) into Milli-Q water to achieve an approximate concentration of 1000±100 µg/L of each micropollutant. Milli-Q water was used to establish thermodynamic profiles related to adsorption between specific micropollutants and biochar, which requires minimizing interference from other constituents that would be present in wastewater. The micropollutant concentrations for batch tests were higher than environmentally relevant concentrations (in the range of ng/L to µg/L [3,42]) such that micropollutant adsorption capacities could be determined via liquid chromatography-mass spectrometry (LC-MS; detection limits were in the 10 µg/L range, as shown in Table S1 in the Supplementary Information). The volumetric ratio of methanol stock to water was below 0.5%, which negates co-solvent effects [44]. The initial water pH was adjusted to 7 using 1 N HCl and 1 N NaOH. The bulk solution pH decreased approximately 1 pH unit over the course of testing, likely due to the intrinsic HCl biochar surface acidity.

Table 1. Physical and chemical properties of the micropollutants in this study. Property data were adapted from PubChem and ChemSpider

Compound	Molecular Structure	pK_a	$logK_{ow}$[b]	$logK_{hw}$[d]	Aqueous solubility mg/L	Polarity
BAC-C10		N/A[a]	N/A[a]	N/A[a]	≥10000	polar
CBZ		13.9	2.45	2.53	112	polar
E2		10.8	3.94	4.33	3.60	non-polar
EE2		10.3	3.67	4.01	11.3	moderately polar
TCS		7.9	4.76[c]	5.33	10.0	non-polar

a No pK_a and $logK_{ow}$ values because BAC-C10 dissociates immediately and because it is an amphiphile.
b log K_{ow} is shown because the majority of analyte molecules are neutral at pH 7 and below.
c log D_{ow} at pH 7 for TCS is 4.70.
d log K_{hw} is the hexadecane-water partitioning constant. Values were calculated through the linear relationship between log K_{ow} and log K_{hw} for nonpolar and weakly polar compounds as proposed by Schwarzenbach et al.[44].

Triplicate batch adsorption tests were conducted in silanized 50-mL serum bottles to develop isotherms for the target micropollutants at a range of temperatures. The experimental temperature was maintained at 4, 25, 35, or 50°C (277, 298, 308, or 323 K). At these temperatures, the compounds tested here are thermally stable as the thermo-decomposing of heterocyclics, aromatics, and substituted aromatic compounds occurs at temperatures above 300°C [45]. Biosolids-derived biochar was dosed at 0.12, 0.2, 0.8, 2, or 2.4 g/L to generate isotherms. The serum bottle reactors were mixed end-over-end using a Cole-Parmer (IL, USA) Roto-Torque Variable Speed Rotator. The bottles were mixed for 48 hours to achieve sufficient equilibrium, as shown by Tong et al. [22]. Water samples were collected from the serum bottles and filtered using 0.45 µm PTFE syringe filters (Agela Technologies, Wilmington, DE) prior to subsequent micropollutant analysis using a Shimadzu LC-MS-2020 (method details and limit of detection are provided in Supplemental Information [SI], S1).

2.4 Data analysis

The adsorption capacity of each micropollutant on biochar (Q_e µg/g biochar or mol/g biochar) was calculated using Eq. 1:

$$Q_e = \frac{(C_0 - C_e) \times V}{M} \text{ Eq. 1}$$

where C_0 is the initial concentration of micropollutant (µg/L), C_e is the concentration at equilibrium (µg/L or mol/L), V is the volume of solution (L), and M is the mass of the adsorbent (g). The Q_e and C_e values were used to generate isotherms, which can be used to derive thermodynamic profiles including isosteric heat, standard enthalpy, entropy, and free energy change of adsorption.

The isosteric heat of adsorption (ΔH_{st}) for a given surface loading, Q_e, was derived from the Clausius-Clapeyron equation (Eq. 2) using a plot of $\ln(C_e)$ versus $1/T$ to obtain the slope:

$$\Delta H_{st} = R \frac{d(\ln C_e)}{d(1/T)} \bigg|_{Q_e} \text{ Eq. 2}$$

where ΔH_{st} is the isosteric heat of adsorption (kJ/mol), R is the ideal gas constant (J/mol-K), C_e is the aqueous-phase concentration at equilibrium (mol/L), and T is temperature (K). Each linear curve is denoted as an isostere.

Although the total enthalpy change (ΔH^0) can be derived from isosteric heat of adsorption, limited knowledge of the maximum adsorbent surface loading/coverage prevents direct integration to calculate the total enthalpy change. Alternately, the enthalpy change and entropy change (ΔS^0) of adsorption can be estimated using the van't Hoff equation, as shown in Eq. 3:

$$\ln K_c = -\frac{\Delta H^0}{RT} + \frac{\Delta S^0}{R} \text{ Eq. 3}$$

where K_c is the thermodynamic equilibrium constant, which is related to, but not exactly the same as, the isotherm constant, K [46]. Using the Freundlich constant, K_f, determined via isotherm modeling, Eq. 4 can be used to derive K_c:

$$Kc = \frac{K_f \rho}{1000} \left(\frac{10^6}{\rho}\right)^{1-n} \text{ Eq. 4}$$

where n is a Freundlich constant, and ρ is the density of pure water (1 g/mL) [47]. For linear adsorption, the thermodynamic constant K_c can be obtained by dividing the linear isotherm constant K (L/g) by a factor of 1,000

g/L [48]. In accordance with Eq. 3, a linear curve can then be plotted for ln(K_c) versus 1/T, wherein the enthalpy change can be estimated from the slope, and the entropy change can be estimated from the y-axis intercept.

The free energy change of adsorption (ΔG^0) was estimated using Eq. 5:

$$\Delta G^0 = -RTlnK_c \quad \text{Eq. 5}$$

Linear regression, correlation, non-linear fitting, and significance of difference analysis (ANOVA, $\alpha \leq 0.05$) were performed using GraphPad Prism 6 (La Jolla, CA, USA).

3. Results and Discussion

3.1 Single-solute adsorption equilibrium and the impact of temperature

Bench-scale batch experiments were conducted to determine the adsorption capacities for micropollutants on biosolids-derived biochar by producing isotherms at a range of reaction temperatures (Figure 1). The Freundlich, Langmuir, or linear isotherm models were tested for all compounds. The BAC-C10, CBZ, and EE2 isotherms fit best to the linear isotherm (SI S2, Table S2). The E2 and TCS isotherms fit best to the Freundlich isotherm. Thermodynamic parameters were derived using the best-fit isotherm.
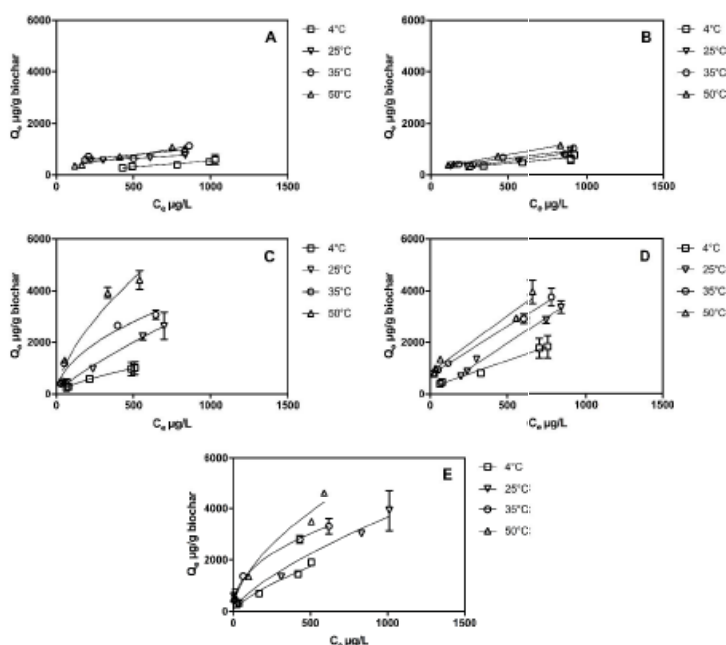
Figure 1. Linear 228 isotherms for A) BAC-C10 , B) CBZ, and D) EE2, and Freundlich isotherms for C) E2 and E) TCS at 4, 25, 35, and 50°C (277, 298, 308, and 323 K, respectively). The adsorption equilibrium of each compound was obtained in a single-solute batch-mode adsorption system. The data represent average results and error bars show ±1 standard deviation of triplicate experiments. Some error bars are small and not visible.

For the aqueous-phase concentration range tested, BAC-C10 and CBZ had much lower equilibrium Q_e values than E2, EE2, and TCS, indicating poorer adsorption under these conditions. The BAC-C10 molecule has a hydrophobic hydrocarbon chain linked to a positively charged nitrogen atom that is also bonded to a benzyl group (Table 1) [49]. The existence of both hydrophobic (benzene) and hydrophilic (N-benzyl group) moieties defines the amphiphilic nature of BAC-C10 as a surfactant. In bulk aqueous phase, the molecules tend to form aggregates, i.e., micelles, with hydrocarbon chains pointing towards the center and the hydrophilic heads in contact with the surrounding water. The low adsorption capacities of BAC C10 could be attributed to the effect

of the hydrophilic moiety. Among the neutral compounds tested, CBZ has the lowest hydrophobicity and the highest solubility in water (Table 1), which could explain its low adsorption capacities.

Interestingly, the degree of linearity of the adsorption isotherm was related to compound polarity. TCS and E2, with non-linear adsorption, are relatively non-polar [50]. The compounds with linear adsorption isotherms, i.e., BAC-C10, CBZ, and EE2, are more polar molecules. One explanation for this trend is that when organic compounds are present at low concentrations (<mg/L), biochar exhibits linear adsorption on its more polar amorphous organic matter fraction and non-linear uptake on the non-polar char fractions [40,51,52] The polar moieties of biochar such as aliphatic and oxygen-containing functional groups could be more accessible for BAC-C10, CBZ, and EE2 via H-bonding or partitioning into the non-carbonized phase. The non-polar and more aromatic moieties of biochar can potentially favor adsorption for more non-polar TCS and E2 via π-interactions [53]. However, the aromatic structures in BAC-C10, CBZ, and EE2 might induce π-system related interactions as well[54]. Hence, linear adsorption could be an integrated effect of interactions with polar and non-polar moieties. Linear adsorption on the amorphous fraction of biochar is relatively weak (lower affinity) compared to non-linear adsorption[52], which is reflected in the magnitude of ΔH^0.

In general, increasing temperature increased the distribution constant, K, of the isotherms (SI S2, Table S2). For the same equilibrium aqueous-phase concentration, higher temperature favors greater adsorption and stronger affinity of the target compounds on the biochar, indicating more energy input was required for these reactions. This result indicates that adsorption of these organic micropollutants from water onto biosolids-derived biochar was endothermic. Estimation of ΔH^0 can quantitatively establish the endothermic nature of this adsorption process.

3.2 Estimation of thermodynamic parameters for single-solute adsorption

The ΔH_{st} of adsorption is the differential heat of adsorption at a fixed surface loading (or adsorption capacity) at equilibrium. Variation in ΔH_{st} with surface loading indicates surface energy heterogeneity. All ΔH_{st} values were positive, further supporting the positive impact of temperature on adsorption (Figure 2 and Table S3), and indicating that adsorption of organic micropollutants from the aqueous phase onto biosolids-derived biochar was an endothermic process. The linear curves of $\ln(C_e)$ over $1/T$ (isosteres) at varied surface loadings are shown in SI S3, Figure S1, and the calculated isostere parameters are shown in Table S3. The average values of isosteric heat decreased as adsorbate surface loading increased. Isosteric heat is associated with adsorption site binding affinity for a given surface loading. Thus, the decrease in isosteric heat suggests that, at low surface loading, high-affinity adsorption sites were initially occupied, absorbing more heat than low-affinity adsorption sites. Low-affinity adsorption sites that absorb less heat were then able to bind the adsorbate as the surface coverage gradually increased. Biosolids-derived biochar therefore features heterogeneous binding sites capable of adsorbing the target micropollutants, which rationalizes the use of the Freundlich isotherm to characterize heterogeneous site distribution across adsorbent surface [55].
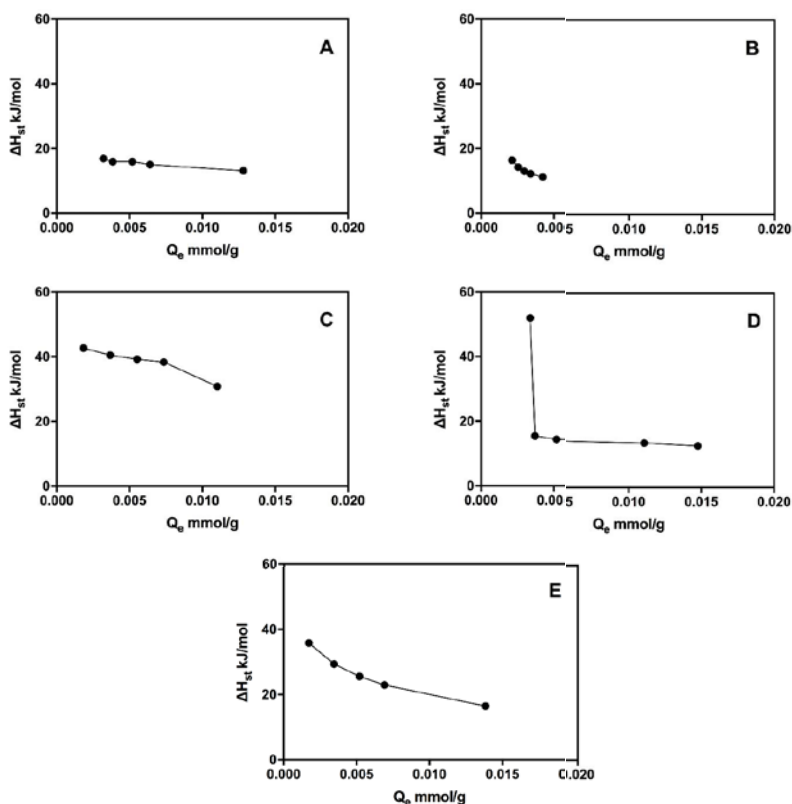
Figure 2. Isosteric heat change (ΔH_{st}) as a function of surface loading (Q_e) for A) BAC-C10, B) CBZ, C) E2, D) EE2, and E) TCS in a single-solute adsorption system. The data represent average results and error bars show ±1 standard deviation of triplicate experiments.

More drastic changes in isosteric heat distribution across the surface loading range were observed for the non-polar micropollutants E2 and TCS. The Freundlich parameter n is an indicator of binding affinity distribution on an adsorbent surface. When n is less than 1, the binding affinity changes more drastically across the adsorbent surface [55]. As previously mentioned, linear adsorption of polar compounds on the amorphous fraction of biochar is usually characterized by weaker affinity. Linear adsorption explains the lower isosteric heats of BAC C10 and CBZ compared to E2 and TCS. The isosteric heat of EE2 decreased sharply for low surface loading, but the rate of change slowed as surface loading increased. The isosteric heat change could stem from EE2 being less polar compared to BAC-C10 and CBZ, which allowed a fraction of the molecules to adsorb on biochar's heterogeneous fraction first. This resulted in more drastic changes in isosteric heat for low surface coverage, while the majority of the EE2 molecules exhibited less heterogeneous linear adsorption as the coverage increased.

The ΔH^0, ΔG^0, and ΔS^0 of single-solute adsorption are related to the thermodynamic equilibrium constant K_c via the van't Hoff equation (SI S4, Figure S2). The experimentally derived values are shown in Table 2. The ΔH^0 of adsorption is the average of the integrated isosteric heat over the maximum surface loading/coverage [56]. The ΔH^0 provides information regarding the adsorption mechanism. For weak intermolecular forces (e.g., H-bond or π-interactions), the change in enthalpy is much less than that for stronger chemical adsorption (which is usually on the order of hundreds of kJ/mol) [57,58], wherein covalent bonds are formed. The estimated ΔH^0 values, which signify the total binding energy per unit of adsorption for the micropollutants, were all positive, signifying the endothermic nature of adsorption from the aqueous phase onto biosolids-derived biochar. Endothermic adsorption is often observed for aqueous/carbonaceous solid adsorption systems [59,60], although it is rare for gas/carbonaceous solid adsorption systems [58].

The endothermic nature of adsorption may be due to 1) overcoming interactions with water molecules, as is the case for weak physical adsorption, or 2) the formation of covalent bonds during chemical adsorption. In the case of aqueous-phase adsorption, heat-consuming endothermic physical adsorption can occur if water molecules interact with the adsorbate or adsorbent via H bonds, and these interactions must be overcome before the adsorbate can adhere onto the adsorbent. The heat-consuming steps that must be overcome can include adsorbate diffusion in the water matrix, which has to break hydrogen bonds formed among water molecules [53,59]; adsorbate diffusion in adsorbent pores [61,62]; and/or the adsorbate replacing pre-adsorbed water molecules, which also needs heat input to break hydrogen bonds between water molecules and the adsorbent. Alternatively, if the formation of covalent bonds is the dominant mechanism, the absolute value of the change of enthalpy should be on the order of 10^2 kJ/mol [58,63]. Adsorption enthalpy changes were one order of magnitude less than the realm of chemisorption, indicating the dominant role of non-covalent physical adsorption. Among the tested compounds, those characterized by linear adsorption, BAC-C10, CBZ, and EE2, experienced less change in enthalpy (12.2, 8.3 and 11.7 kJ/mol, respectively) in comparison to E2 and TCS (48.9 and 81.4 kJ/mol, respectively), which were better characterized by stronger non-linear adsorption.

The sum of a number of intermolecular interactions contributes to the total free energy change (ΔG^0) of adsorption. Usually the ΔG^0 for adsorption is negative, signifying the spontaneity of the attachment [64]. The entire process for solutes diffusing and adsorbing onto sites was spontaneous, as demonstrated by the negative ΔG^0 (Table 2). The experimentally determined $|\Delta G^0|$ values (listed in Table 2) agree with previous studies that organic micropollutant adsorption on plant derived biochar could be on the order of 10 kJ mol^{-1} or less, and rarely exceeds 50 kJ mol^{-1} [53,65,66].

The entropy change (ΔS^0) indicates the disorder of the adsorption system. Hydrophobic interactions between adsorbent and adsorbate are primarily driven by the tendency of the adsorption system to gain entropy [40,67]. The adsorbed-phase compounds had greater entropy than the aqueous-phase compounds, as demonstrated by the positive ΔS^0 value. The gain in entropy denotes the existence of non-specific hydrophobic interactions between the organic molecules or micelles and the biochar surface [40,67]. For the neutral compounds CBZ, E2, EE2, and TCS, the increase in entropy (ΔS^0) was positively correlated to logK_{ow} values (linear regression correlation coefficient R^2=0.8), implying that non-specific hydrophobic interaction could play an important role in neutral molecule adsorption [54].

Table 2. Experimentally derived changes in Gibbs free energy (ΔG^0), enthalpy (ΔH^0), and entropy (ΔS^0) for adsorption of micropollutants to biosolids-derived biochar under single-solute conditions.

Compound	Temperature K	ΔG^0 kJ/mol	ΔH^0 kJ/mol	$T\Delta S^0$ kJ/mol	ΔS^0 J/mol/K
BAC-C10	277	-14.2	12.2	25.6	93.0
	298	-14.6		27.7	
	308	-16.3		28.6	
	323	-18.6		30.0	
CBZ	277	-14.7	8.3	22.9	82.8
	298	-16.6		24.4	
	308	-16.8		25.3	
	323	-18.7		26.5	
E2	277	-17.4	48.9	64.3	232
	298	-12.8		69.1	
	308	-28.9		71.5	
	323	-25.6		75.0	
EE2	277	-17.6	11.7	29.4	107
	298	-20.6		31.6	
	308	-21.1		32.6	
	323	-22.5		34.2	
TCS	277	-15.6	81.4	96.7	349

	298	-18.1		104	
	308	-33.8		108	
	323	-28.3		113	

3.3 Impact of micropollutant competition on thermodynamic profiles

In general, for competition stemming from multi-solute conditions, increasing temperature increased adsorption of the micropollutants (similar to single-solute conditions). But competitive adsorption had less impact for BAC-C10 at low temperatures (Figure 3). As was the case for single-solute conditions, the Freundlich isotherm provided a better fit for E2 and TCS (Figures 3C and 3E, respectively, fitting parameters in SI S5), while the linear isotherm provided a better fit for BAC-C10, CBZ, and EE2 (Figures 3A, 3B and 3D, respectively) adsorption in multi solute conditions. For linear isotherms at 4°C and 25°C, BAC-C10 had low Q_e values and poor fit. The poor isotherm fits and negligible impact of low temperatures on BAC-C10 adsorption could stem from the competition effect from other compounds. Due to its hydrophilic nature, adsorption of BAC-C10 molecules could be more susceptible to competitive adsorption. For the temperatures tested, EE2 adsorption in multi-solute conditions was inhibited, as shown by the significant decrease in the linear distribution coefficient ($p < 0.05$). The E2 multi-solute isotherm parameters also differed from the single-solute isotherms, with a significantly lower Freundlich constant K_f ($p < 0.05$). TCS was a stronger competitor for adsorption sites than EE2 and E2. Past research attributed different competitive behaviors to micropollutant hydrophobicity [68,69]. The greater the hydrophobicity of the micropollutant, the stronger competition behavior it exhibits under multi-solute adsorption [69,70].

Suppressed adsorption due to competition was not ubiquitous for all micropollutants (SI S6, Table S5). For CBZ and TCS, adsorption was not significantly affected by multi-solute competition at the tested temperatures (ANOVA, $p > 0.05$), indicating that it preferentially adsorbed to biochar and outcompeted other solutes. The competitive behavior of CBZ whereby CBZ adsorption remains unchanged in mixed solute conditions could be attributed to its higher polarity compared with other neutral co-solutes. Chiou and Kile[71] found that nonlinear sorption of a non-polar solute (trichloroethylene) was largely suppressed by polar molecules such as phenol and 3,5-dichlorophenol. The suppression effect that the polar CBZ molecule has on other solutes could be attributed accordingly. The competitive adsorption of polar CBZ suggested that multiple mechanisms could account for the polar interactions, among which H-bonds in between CBZ and polar moieties of biochar might outcompete non-specific hydrophobic interaction for adsorption sites. Future research is needed to be able to distinguish the contributions of mechanisms for polar aromatic compound adsorption.
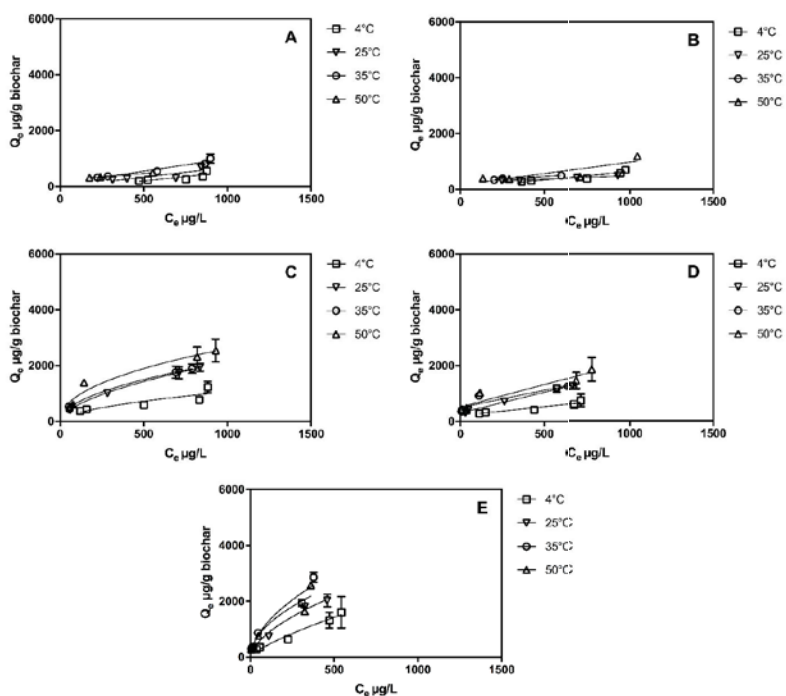
Figure 3. Multi-solute system adsorption linear isotherms for A) BAC-C10, B) CBZ, and D) EE2 and Freundlich isotherms for C) E2 and E) TCS at 4, 25, 35, and 50°C (277, 298, 308, and 323 K, respectively). The data represent average results and error bars show ±1 standard deviation of triplicate experiments. Some error bars are small and not visible.

Competitive adsorption did not change the endothermic nature of adsorption, nor the heterogeneous distribution of binding sites on the biochar's surface, according to the isosteric heat with surface loading plots under competitive adsorption (Figure 4). Negative ΔG^0 for all reactions indicated that the competitive adsorption reactions were spontaneous for the temperatures tested (Table 3).

Comparison of the van't Hoff curves (SI S8, Figure S4), which were generated from isostere curves (SI S6) showed that the ΔH^0 and ΔS^0 for all compounds were not significantly altered by competitive adsorption in multi-solute conditions (SI S9, Table S7, p>0.05). However, multi solute competition decreased some adsorption capacities to differing extents. As demonstrated here, the binding energy (enthalpy change) and extent of disorder (entropy change) are inherent thermodynamic properties of a reaction and are closely related to the thermodynamic equilibrium constant. Accordingly, only changes in reaction activation energy or physical states of the adsorbent and adsorbate can impact thermodynamic properties of adsorption [72].
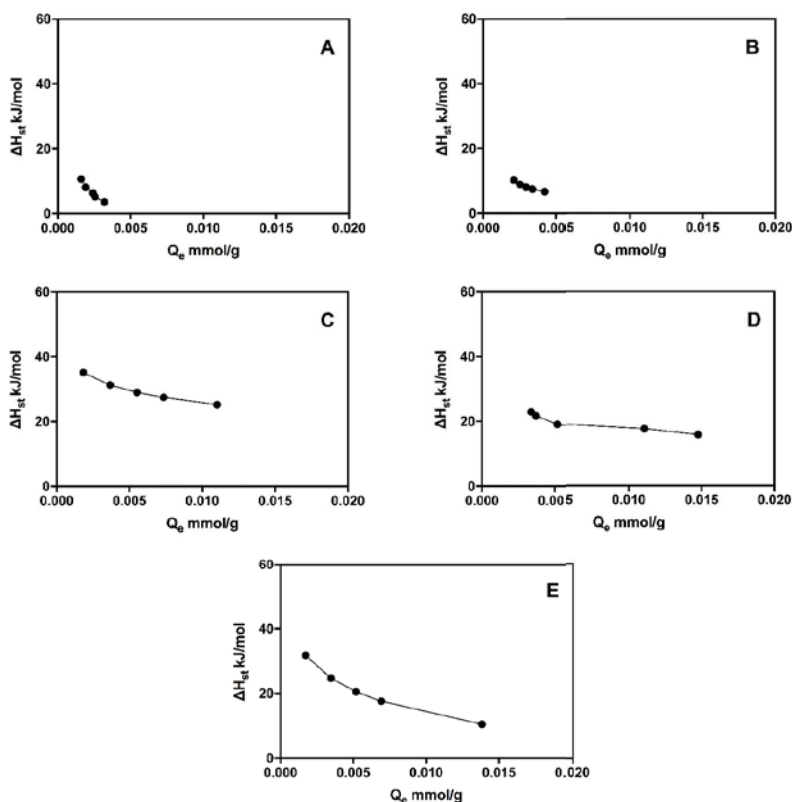
Figure 4. Isosteric heat change (ΔH_{st}) with surface loading (Q_e) for A) BAC-C10, B) CBZ, C) E2, D) EE2, and E) TCS, in multi-solute conditions. The data represent average results and error bars show ± 1 standard deviation of triplicate experiments.

Table 3. Experimentally derived changes in Gibbs free energy (ΔG^0), enthalpy (ΔH^0), and entropy (ΔS^0) for micropollutant adsorption under multi-solute conditions.

Compound	Temperature K	ΔG^0 kJ/mol	ΔH^0 kJ/mol	$T\Delta S^0$ kJ/mol	ΔS^0 J/mol/K
BAC-C10	277	-14.8	7.7	22.5	81.1
	298	-16.2		24.2	
	308	-17.5		25.0	
	323	-16.6		26.2	
CBZ	277	-14.6	4.2	17.9	64.7
	298	-13.5		19.3	
	308	-15.1		19.9	
	323	-18.0		20.9	
E2	277	-20.7	52	71.4	258
	298	-21.0		76.8	
	308	-29.4		79.4	
	323	-31.9		83.2	
EE2	277	-14.9	14	29.4	106
	298	-18.1		31.6	
	308	-18.2		32.7	
	323	-19.8		34.3	
TCS	277	-14.0	90	105	378
	298	-23.8		113	
	308	-27.4		116	
	323	-30.8		122	

4. Conclusions

This research demonstrated that biosolids-derived biochar adsorbed a suite of micropollutants, albeit to differing extents. More polar compounds such as BAC-C10 and CBZ exhibited more linear adsorption with higher Freundlich isotherm n values, indicating weak interactions with more polar amorphous biochar moieties. For the neutral micropollutants, increasing hydrophobicity increased the extent of adsorption. Accordingly, the most hydrophobic compound tested, TCS, had the highest adsorption capacity under the experimental conditions. The ΔH^0 value of adsorption, strong Freundlich isotherm fits, and the positive correlation between hydrophobicity (log K_{ow} or log K_{hw}) and ΔS^0 all suggest weak physical binding and that hydrophobic interaction is the dominant mechanism. This knowledge indicates that biosolids derived biochar has higher removal efficiency of neutral and hydrophobic contaminants. Future research should focus on optimizing biochar's surface to improve adsorption of polar contaminants.

Estimation of the thermodynamic parameters of adsorption indicated that all of the adsorption reactions were endothermic. The positive impact of temperature also signified that biochar adsorbs better at elevated water temperatures. Thus, in water treatment applications, adsorption is likely higher in warmer seasons or climates.

The negative ΔG^0 values suggest spontaneous adsorption of the target micropollutants using biosolids-derived biochar. It is unlikely that the reverse reaction, i.e., desorption, would outcompete adsorption. Therefore, the adsorbed micropollutants will not detach from the biochar, unless processes with external energy input are applied, such as pyrolysis or combustion.

Under multi-solute conditions, E2 and EE2 adsorption was suppressed, while TCS adsorption was unaffected, indicating biosolids-derived biochar's preference for adsorption of more hydrophobic compounds. Adsorption of CBZ was essentially unaffected under the multi-solute condition, likely due to its enhanced competitiveness based on its polarity. Parameters reflecting thermodynamic properties, such as binding energy and ΔS^0, were not affected by the presence or absence of other solutes in the matrix. It is expected that lower adsorption capacities would be observed in a wastewater matrix, wherein greater competition for adsorption sites would be encountered. However, the matrix cannot change thermodynamic properties, i.e., mechanisms of adsorption.

Evaluating the impact of water temperature and the thermodynamic profile of adsorption is beneficial for understanding the factors limiting adsorption and in guiding optimization of engineering parameters for micropollutant removal through adsorption on biosolids-derived biochar. Linking thermodynamic parameters with micropollutant properties such as hydrophobicity can provide predictive information for assessing the feasibility and extent of removal of a contaminant by biochar. Future research should focus on quantitative correlations between the adsorption thermodynamics and biochar surface properties, such as binding site distribution, which would be beneficial in engineering biochar surface chemistry for optimized micropollutant removal. Additional research could be conducted using biochars produced at different temperatures.

Acknowledgements

References

1 B. D. Blair, Potential Upstream Strategies for the Mitigation of Pharmaceuticals in the Aquatic Environment: a Brief Review, *Curr. Environ. Heal. reports*, 2016, 3, 153–160.

2 T. Rauch-Williams, S. Snyder, J. Drewes and E. Dickinson, Current and Proposed Paradigms to Control CECs in the United States and Internationally: Phase 1 Report, 2016, 102.

3 B. D. Blair, J. P. Crago, C. J. Hedman and R. D. Klaper, Pharmaceuticals and personal care products found in the Great Lakes above concentrations of environmental concern, *Chemosphere*, 2013, 93, 2116–2123.

4 M. R. Servos, D. T. Bennie, B. K. Burnison, A. Jurkovic, R. McInnis, T. Neheli, A. Schnell, P. Seto, S. A. Smyth and T. A. Ternes, Distribution of estrogens, 17beta estradiol and estrone, in Canadian municipal wastewater treatment plants, *Sci. Total Environ.*, 2005, 336, 155–70.

5 E. Silva, N. Rajapakse and A. Kortenkamp, *Environ. Sci. Technol.*, Something from "nothing" - Eight weak estrogenic chemicals combined at concentrations below NOECs produce significant mixture effects, 2002, 36, 1751–1756.

6 A. M. Vajda, L. B. Barber, J. L. Gray, E. M. Lopez, A. M. Bolden, H. L. Schoenfuss and D. O. Norris, Demasculinization of male fish by wastewater treatment plant effluent, *Aquat. Toxicol.*, 2011, 103, 213–21.

7 A. M. Vajda, L. B. Barber, J. L. Gray, E. M. Lopez, J. D. Woodling and D. O. Norris, Reproductive disruption in fish downstream from an estrogenic wastewater effluent, *Environ. Sci. Technol.*, 2008, 42, 3407–14.

8 D. E. Carey, D. H. Zitomer, A. D. Kappell, M. J. Choi, K. R. Hristova and P. J. McNamara, Chronic exposure to triclosan sustains microbial community shifts and alters antibiotic resistance gene levels in anaerobic digesters, *Environ. Sci. Process. Impacts*, 2016, 18, 1060–1067.

9 R. P. Schwarzenbach, B. I. Escher, K. Fenner, T. B. Hofstetter, C. A. Johnson, U. von Gunten and B. Wehrli, The challenge of micropollutants in aquatic systems, *Science*, 2006, 313, 1072–1077.

10 P. J. Vikesland, A. Pruden, P. J. J. Alvarez, D. Aga, H. Bürgmann, X. D. Li, C. M. Manaia, I. Nambi, K. Wigginton, T. Zhang and Y. G. Zhu, Toward a Comprehensive Strategy to Mitigate Dissemination of Environmental Sources of Antibiotic Resistance, *Environ. Sci. Technol.*, 2017, 51, 13061–13069.

11 D. E. Carey and P. J. Mcnamara, The impact of triclosan on the spread of antibiotic resistance in the environment, *Front. Microbiol.*, 2015, 5.

12 D. E. Carey, D. H. Zitomer, K. R. Hristova, A. D. Kappell and P. J. McNamara, Triclocarban Influences Antibiotic Resistance and Alters Anaerobic Digester Microbial Community Structure, *Environ. Sci. Technol.*, 2016, 50, 126–134.

13 D. E. Carey and P. J. McNamara, Altered antibiotic tolerance in anaerobic digesters acclimated to triclosan or triclocarban, *Chemosphere*, 2016, 163, 22–26.

14 K. Kimura, G. Amy, J. E. Drewes, T. Heberer, T.-U. Kim and Y. Watanabe, Rejection of organic micropollutants (disinfection by-products, endocrine disrupting compounds, and pharmaceutically active compounds) by NF/RO membranes, *J. Memb. Sci.*, 2003, 227, 113–121.

15 M. Carballa, F. Omil, T. Ternes and J. M. Lema, Fate of pharmaceutical and personal care products (PPCPs) during anaerobic digestion of sewage sludge, *Water Res.*, 2007, 41, 2139–2150.

16 B. M. K. Manda, E. Worrell and M. K. Patel, Innovative membrane filtration system for micropollutant removal from drinking water – prospective environmental LCA and its integration in business decisions, *J. Clean. Prod.*, 2014, 72, 153–166.

17 E. Kim, C. Jung, J. Han, N. Her, C. Min Park, A. Son and Y. Yoon, Adsorption of selected micropollutants on powdered activated carbon and biochar in the presence of kaolinite, *Desalin. Water Treat.*, 2016, 57, 27601–27613.

18 J. Margot, C. Kienle, A. Magnet, M. Weil, L. Rossi, L. F. de Alencastro, C. Abegglen, D. Thonney, N. Chèvre, M. Schärer and D. A. Barry, Treatment of micropollutants in municipal wastewater: ozone or powdered activated carbon? *Sci. Total Environ.*, 2013, 461–462, 480–98.

19 C. Jung, J. Park, K. H. Lim, S. Park, J. Heo, N. Her, J. Oh, S. Yun and Y. Yoon, Adsorption of selected endocrine disrupting compounds and pharmaceuticals on activated biochars, *J. Hazard. Mater.*, 2013, 263 Pt 2, 702–10.

20 Y. Wang, J. Lu, J. Wu, Q. Liu, H. Zhang and S. Jin, Adsorptive removal of fluoroquinolone antibiotics using bamboo biochar, *Sustain.*, 2015, 7, 12947–12957.

21 M. Ahmad, S. S. Lee, S. E. Oh, D. Mohan, D. H. Moon, Y. H. Lee and Y. S. Ok, Modeling adsorption kinetics of trichloroethylene onto biochars derived from soybean stover and peanut shell wastes, *Environ. Sci. Pollut. Res.*, 2013, 20, 8364–8373.

22 Y. Tong, B. K. Mayer and P. J. McNamara, Triclosan adsorption using wastewater biosolids-derived biochar, *Environ. Sci. Water Res. Technol.*, 2016, 2, 761–768.

23 Z. Liu, S. Singer, Y. Tong, L. Kimbell, E. Anderson, M. Hughes, D. Zitomer and P. McNamara, Characteristics and applications of biochars derived from wastewater solids, *Renew. Sustain. Energy Rev.*, 2018, 90, 650–664.

24 K. A. Thompson, K. K. Shimabuku, J. P. Kearns, D. R. U. Knappe, R. S. Summers and S. M. Cook, Environmental comparison of biochar and activated carbon for tertiary wastewater treatment, *Environ. Sci. Technol.*, 2016, 50, 11253–11262.

25 K. K. Shimabuku, J. P. Kearns, J. E. Martinez, R. B. Mahoney, L. Moreno-Vasquez and R. S. Summers, Biochar sorbents for sulfamethoxazole removal from surface water, stormwater, and wastewater effluent, *Water Res.*, 2016, 96, 236–245.

26 B. G. Greiner, K. K. Shimabuku and R. S. Summers, Influence of biochar thermal regeneration on sulfamethoxazole and dissolved organic matter adsorption, *Environ. Sci. Water Res. Technol.*, 2018, 4, 169–174.

27 Y. Tong, L. K. Kimbell, A. Avila, P. J. McNamara and B. K. Mayer, Ion exchange for nutrient removal coupled with biosolids-derived biochar pretreatment to remove micropollutants, *Environ. Eng. Sci.*, 2018, 35.

28 J. J. Ross, D. H. Zitomer, T. R. Miller, C. A. Weirich and P. J. McNamara, Emerging investigators series: pyrolysis removes common microconstituents triclocarban, triclosan, and nonylphenol from biosolids, *Environ. Sci. Water Res. Technol.*, 2016, 2, 282-289.

29 T. C. Hoffman, D. H. Zitomer and P. J. McNamara, Pyrolysis of wastewater biosolids significantly reduces estrogenicity, *J. Hazard. Mater.*, 2016, 317, 579–584.

30 L. K. Kimbell, A. D. Kappell and P. J. McNamara, Effect of pyrolysis on the removal of antibiotic resistance genes and class I integrons from municipal wastewater biosolids, *Environ. Sci. Water Res. Technol.*, 2018, 4, 1807-1818.

31 D. E. Carey, P. J. McNamara and D. H. Zitomer, Biochar from Pyrolysis of Biosolids for Nutrient Adsorption and Turfgrass Cultivation, *Water Environ. Res.*, 2015, 87, 2098–2106.

32 J. Lehmann, J. Gaunt and M. Rondon, Bio-char Sequestration in Terrestrial Ecosystems – A Review, *Mitigation and Adaptation Strategies for Global Change*, 2006, 11, 395–419.

33 P. J. McNamara, J. D. Koch, Z. Liu and D. H. Zitomer, Pyrolysis of Dried Wastewater Biosolids Ca n Be Energy Positive, *Water Environ. Res.*, 2016, 88, 804–810.

34 P. McNamara, J. Koch and D. Zitomer, Pyrolysis of wastewater biosolids: lab-scale experiments and modeling, *Proc. Water Environ. Fed.*, 2014, 2014, 1–14.

35 H. Yao, J. Lu, J. Wu, Z. Lu, P. C. Wilson and Y. Shen, Adsorption of fluoroquinolone antibiotics by wastewater sludge biochar: Role of the sludge source, *Water. Air. Soil Pollut.*, 2013, 224.

36 W. Zheng, M. Guo, T. Chow, D. N. Bennett and N. Rajagopalan, Sorption properties of greenwaste biochar for two triazine pesticides, *J. Hazard. Mater.*, 2010, 181, 121–126.

37 D. K. Mahmoud, M. A. M. Salleh, W. A. W. A. Karim, A. Idris and Z. Z. Abidin, Batch adsorption of basic dye using acid treated kenaf fibre char: Equilibrium, kinetic and thermodynamic studies, *Chem. Eng. J.*, 2012, 181–182, 449–457.

38 F. Lian, B. Sun, Z. Song, L. Zhu, X. Qi and B. Xing, *Chem. Eng. J.*, 2014, 248, 128–134.

39 M. Vithanage, S. S. Mayakaduwa, I. Herath, Y. S. Ok and D. Mohan, *Chemosphere*, 2016, 150, 781–789.

40 Z. Chen, B. Chen, D. Zhou and W. Chen, *Environ. Sci. Technol.*, 2012, 46, 12476–12483.

41 B. D. Blair, J. P. Crago, C. J. Hedman, R. J. F. Treguer, C. Magruder, L. S. Royer and R. D. Klaper, *Sci. Total Environ.*, 2013, 444, 515–21.

42 V. M. Monsalvo, J. A. McDonald, S. J. Khan and P. Le-Clech, Removal of trace organics by anaerobic membrane bioreactors, *Water Res.*, 2014, 49, 103–112.

43 L. K. Kimbell, Y. Tong, B. K. Mayer and P. J. McNamara, Biosolids-Derived Biochar for Triclosan Removal from Wastewater, *Environ. Eng. Sci.*, 2017, ees.2017.0291.

44 R. P. Schwarzenbach, P. M. Gschwend and D. M. Imboden, *Environmental organic chemistry*, John Wiley & Sons, 2005.

45 I. B. Johns, E. A. McElhill and J. O. Smith, Thermal Stability of Some Organic Compounds, *J. Chem. Eng. Data*, 1962, 7, 277–281.

46 H. N. Tran, S. J. You, A. Hosseini-Bandegharaei and H. P. Chao, Mistakes and inconsistencies regarding adsorption of contaminants from aqueous solutions: A critical review, *Water Res.*, 2017, 120, 88–116.

47 P. S. Ghosal and A. K. Gupta, An insight into thermodynamics of adsorptive removal of fluoride by calcined Ca–Al–(NO 3) layered double hydroxide, *RSC Adv.*, 2015, 5, 105889–105900.

48 S. K. Milonjić, A consideration of the correct calculation of thermodynamic parameters of adsorption, *J. Serbian Chem. Soc.*, 2007, 72, 1363–1367.

49 E. Martínez-Carballo, A. Sitka, C. González-Barreiro, N. Kreuzinger, M. Fürhacker, S. Scharf and O. Gans, Determination of selected quaternary ammonium compounds by liquid chromatography with mass spectrometry. Part I. Application to surface, waste and indirect discharge water samples in Austria, *Environ. Pollut.*, 2007, 145, 489–496.

50 R. C. Petersen, Triclosan Computational Conformational Chemistry Analysis for Antimicrobial Properties in Polymers, *J. Nat. Sci.*, 2015, 1, e54.

51 B. Chen, D. Zhou and L. Zhu, Transitional adsorption and partition of nonpolar and polar aromatic contaminants by biochars of pine needles with different pyrolytic temperatures, *Environ. Sci. Technol.*, 2008, 42, 5137–5143.

52 J. Lehmann and J. Stephen, *Biochar for Environmental Management: Science And Technology*, 2009, vol. 1.

53 Y. Tong, P. J. McNamara and B. K. Mayer, Adsorption of organic micropollutants onto biochar: a review of relevant kinetics, mechanisms and equilibrium, *Environ. Sci. Water Res. Technol.*, 2019, DOI: 10.1039/C8EW00938D.

54 M. Kah, G. Sigmund, F. Xiao and T. Hofmann, Sorption of ionizable and ionic organic compounds to biochar, activated carbon and other carbonaceous materials, *Water Res.*, 2017, 124, 673–692.

55 M. M. Benjamin and D. F. Lawler, *Water Quality Engineering: Physical / Chemical Treatment Processes*, Wiley, 2013.

56 K. S. W. Sing, D. H. Everett, R. A. W. Haul, L. Moscou, R. A. Pierotti, J. Rouquero and T. S. Reporting physisorption data for gas/solid systems with special reference to the determination of surface area and porosity, *Pure appl. Chem.*, 1985, 57, 603–619.

57 S. Chowdhury, R. Mishra, P. Saha and P. Kushwaha, Adsorption thermodynamics, kinetics and isosteric heat of adsorption of malachite green onto chemically modified rice husk, *Desalination*, 2011, 265, 159–168.

58 J. M. Thomas, The existence of endothermic adsorption, *J. Chem. Educ.*, 1961, 38, 138.

59 M. A. Fontecha-Cámara, M. V. López-Ramón, M. A. Álvarez-Merino and C. Moreno-Castilla, About the endothermic nature of the adsorption of the herbicide diuron from aqueous solutions on activated carbon fiber, *Carbon N. Y.*, 2006, 44, 2335–2338.

60 V. C. Srivastava, I. D. Mall and I. M. Mishra, *Chem. Eng. J.*, 2007, 132, 267–278.

61 T. S. Anirudhan and P. G. Radhakrishnan, Adsorption thermodynamics and isosteric heat of adsorption of toxic metal ions onto bagasse fly ash (BFA) and rice husk ash (RHA), *J. Chem. Thermodyn.*, 2008, 40, 702–709.

62 J. F. García-Araya, F. J. Beltrán, P. Álvarez and F. J. Masa, Activated carbon adsorption of some phenolic compounds present in agroindustrial wastewater, *Adsorption*, 2003, 9, 107–115.

63 P. Saha and S. Chowdhury, Insight Into Adsorption Thermodynamics, *J. Hazard. Mater.*, 2003, 162, 440.

64 R. Zhang and P. Somasundaran, Advances in adsorption of surfactants and their mixtures at solid/solution interfaces, *Adv. Colloid Interface Sci.*, 2006, 123–126, 213–229.

65 Z. Wu, H. Zhong, X. Yuan, H. Wang, L. Wang, X. Chen, G. Zeng and Y. Wu, Adsorptive removal of methylene blue by rhamnolipid-functionalized graphene oxide from wastewater, *Water Res.*, 2014.

66 X. Zhao, W. Ouyang, F. Hao, C. Lin, F. Wang, S. Han and X. Geng, Properties comparison of biochars from corn straw with different pretreatment and sorption behaviour of atrazine, *Bioresour. Technol.*, 2013, 147, 338–344.

67 E. E. Meyer, K. J. Rosenberg and J. Israelachvili, Recent progress in understanding hydrophobic interactions, *Proc. Natl. Acad. Sci. U. S. A.*, 2006, 103, 15739–46.

68 X. Wang, T. Sato and B. Xing, Competitive sorption of pyrene on wood chars, *Environ. Sci. Technol.*, 2006, 40, 3267–3272.

69 Z. Yu and W. Huang, Competitive Sorption between 17α-Ethinyl Estradiol and Naphthalene/Phenanthrene by Sediments, *Environ. Sci. Technol.*, 2005, 39, 4878–4885.

70 B. Pan and B. Xing, Competitive and complementary adsorption of bisphenol a and 17α-ethinyl estradiol on carbon nanomaterials, *J. Agric. Food Chem.*, 2010, 58, 8338–8343.

71 C. T. Chiou and D. E. Kile, Deviations from sorption linearity on soils of polar and nonpolar organic compounds at low relative concentrations, *Environ. Sci. Technol.*, 1998, 32, 338–343.

72 A. Michaelides, Z. P. Liu, C. J. Zhang, A. Alavi, D. A. King and P. Hu, Identification of general linear relationships between activation energies and enthalpy changes for dissociation reactions at surfaces, *J. Am. Chem. Soc.*, 2003, 125, 3704–3705.